

## SCIENTIFIC ARTICLES

# Differential Scanning Calorimetric Studies of Nickel Titanium Rotary Endodontic Instruments

W. A. Brantley, T. A. Svec, M. Iijima, J. M. Powers, and T. H. Grentzer

Differential scanning calorimetric (DSC) analyses were performed between  $-130^{\circ}$  and  $100^{\circ}\text{C}$  on specimens prepared from nickel-titanium (NiTi) rotary endodontic instruments: ProFile ( $n = 5$ ), Lightspeed ( $n = 4$ ), and Quantec ( $n = 3$ ). The ProFile and Lightspeed instruments were in the as-received condition, whereas the Quantec instruments were randomly selected from a dental clinic and had unknown history. The DSC plots showed that the ProFile and Lightspeed instruments analyzed had the superelastic NiTi property, with an austenite-finish ( $A_f$ ) temperature of approximately  $25^{\circ}\text{C}$ . Differences in DSC plots for the ProFile instruments and the starting wire blanks ( $n = 2$ ) were attributed to the manufacturing process. The phase transformation behavior when the specimens were heated and cooled between  $-130^{\circ}$  and  $100^{\circ}\text{C}$ , the temperature ranges for the phase transformations, and the resulting enthalpy changes were similar to those previously reported for nickel-titanium orthodontic wires having superelastic characteristics or shape memory behavior in the oral environment. The experiments demonstrated that DSC is a powerful tool for materials characterization of these rotary instruments, providing direct information not readily available from other analytical techniques about the NiTi phases present, which are fundamentally responsible for their clinical behavior.

After the pioneering research by Walia et al. (1), which introduced nickel-titanium (NiTi) hand files to the endodontic profession, both nickel-titanium hand files and particularly rotary instruments have achieved widespread popularity. A major reason for their selection is the much greater flexibility (i.e. much lower elastic modulus) of the nickel-titanium alloy compared with stainless steel (1), which offers distinct clinical advantages with curved root canals. Numerous articles have recently reported the performance of the different

brands of nickel-titanium rotary instruments (2–6) and hand instruments (7–9).

The manufacture of nickel-titanium instruments for endodontics has been discussed in a review article (10). The nickel-titanium alloys have the approximate composition of 55% nickel and 45% titanium and are based upon the intermetallic compound NiTi (11). Originally introduced for orthodontics (12), the nickel-titanium archwire alloys are available in nonsuperelastic, superelastic, and shape-memory forms (11, 13, 14). The nonsuperelastic nickel-titanium alloys have a predominantly heavily cold-worked, stable, martensitic NiTi structure, whereas the superelastic and shape memory alloys undergo a reversible transformation by twinning on the atomic scale (11) from the lower-temperature martensitic NiTi structure to the higher-temperature austenitic NiTi structure. The superelastic alloys undergo transformation from austenitic NiTi to martensitic NiTi with the application of stress. The shape memory alloys return to a higher-temperature shape established during processing (15), when the temperature is raised above the austenite-finish ( $A_f$ ) temperature, where the transformation to the austenitic NiTi structure is completed. The NiTi shape memory alloys used in orthodontics have the  $A_f$  temperature below body temperature, whereas the superelastic (but not shape memory) orthodontic alloys have the  $A_f$  temperature above that of the oral environment (16). The overall phase transformation process can be complex, and it has been found that an intermediate R-phase can form during the transformation between martensitic and austenitic NiTi (17).

The structure of the NiTi alloys, which is central to their clinical performance, is conveniently studied by differential scanning calorimetry (DSC), in which the difference in thermal power supplied to a test specimen and an inert control specimen heated at the same rate is measured very accurately (11, 16). Structural transformations in the NiTi alloys are revealed as endothermic peaks on the heating DSC curves and as exothermic peaks on the cooling DSC curves, and information is obtained about the temperature ranges and enthalpy changes for the phase transformations. For NiTi alloys, DSC indicates which of the three phases (martensitic NiTi, R-phase, or austenitic NiTi) will be present at a given temperature. Although X-ray diffraction analysis is a useful complementary method to investigate the structure of NiTi orthodontic wires (18), this technique only reveals the structure within approximately  $50\ \mu\text{m}$  of the surface, whereas DSC provides information for the overall bulk specimen (19). Electrical resistivity measurements

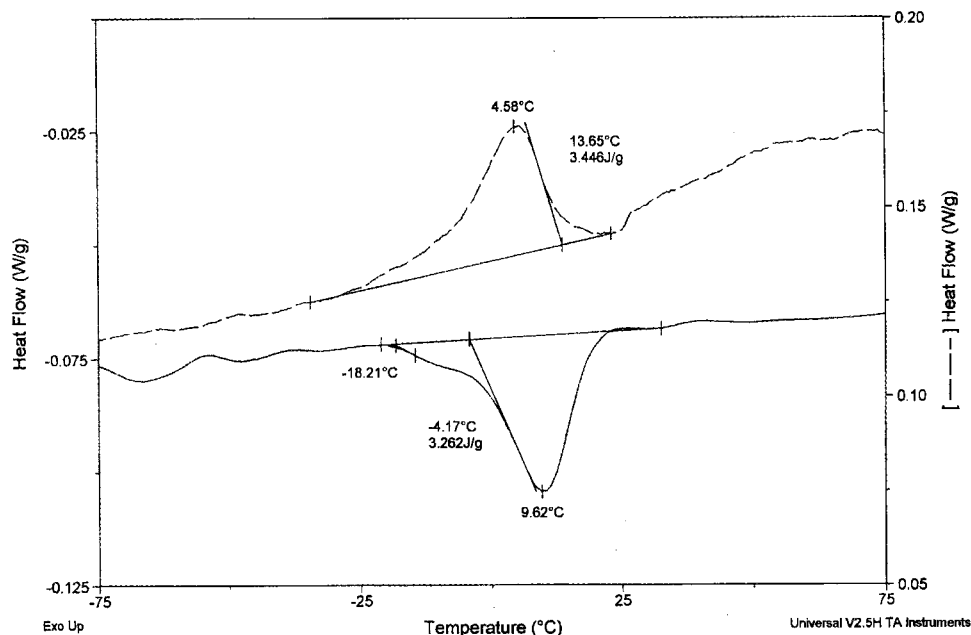


FIG 1. DSC plot for a ProFile specimen. The solid line is the heating curve, and the dashed line is the cooling curve.

may also be used to study the structural transformations in the nickel-titanium alloys (11). The purpose of this study was to utilize DSC to investigate the phase relationships within three brands of popular nickel-titanium rotary endodontic instruments.

## MATERIALS AND METHODS

Three brands of rotary nickel-titanium endodontic instruments (ProFile 0.04 taper, Dentsply Tulsa Dental, Tulsa, OK; Lightspeed, Lightspeed Technology, San Antonio, TX; Quantec, Analytic/Sybron Dental Specialties, Orange, CA) were selected for study, along with starting 1.0-mm diameter wire blanks for the ProFile instruments that were obtained from the manufacturer. Test specimens were carefully cut with a water-cooled, slow-speed diamond saw to minimize mechanical stresses that might change the proportions of the austenitic and martensitic NiTi phases from those in the as-received instruments and wire blanks. Each test specimen consisted of 2 to 4 segments, each approximately 4 to 5 mm in length, which were placed in an open aluminum pan; no crimped pan top was used to avoid mechanical stresses on the specimens. An empty aluminum pan served as the inert control specimen for the DSC measurements.

Five specimens were analyzed for the 25-mm long, ISO size 25 ProFile instruments. Four specimens were randomly selected from a package containing ISO sizes 40, 42.5, 45, and 47.5 for the 25-mm long, Lightspeed instruments. Three specimens were analyzed for the Quantec instruments, which were of varying sizes and randomly selected from the Endodontic Clinic at the University of Texas-Houston Dental Branch. Two replicate specimens of the starting wire blanks for the ProFile instruments were analyzed. The ProFile and Lightspeed instruments were in the as-received condition, whereas the Quantec instruments had an unknown clinical history.

The DSC analyses were conducted (model 2910 DSC, TA Instruments, Wilmington, DE) over a temperature range from  $-130^{\circ}\text{C}$  to  $100^{\circ}\text{C}$ , using the liquid nitrogen cooling accessory (TA

Instruments) to achieve subambient temperatures. For each analysis, the specimen was first cooled from room temperature to  $-130^{\circ}\text{C}$ , then heated from  $-130^{\circ}\text{C}$  to  $100^{\circ}\text{C}$  to obtain the heating DSC curve, and subsequently cooled from  $100^{\circ}\text{C}$  back to  $-130^{\circ}\text{C}$  to obtain the cooling DSC curve. The linear heating or cooling rate was a standard  $10^{\circ}\text{C}$  per minute (16), and during each analysis, the DSC cell was purged with dry nitrogen at a rate of  $50\text{ cm}^3/\text{min}$ . Temperature calibration of the DSC apparatus was performed with n-pentane, deionized water, and indium. The DSC plots were analyzed by computer software (TA Instruments) to obtain the peak temperatures for the phase transformations, along with the enthalpy changes associated with these processes. The interpretations of the plots were based upon previous DSC studies of NiTi alloys in orthodontics (11, 16, 20).

## RESULTS

Figures 1 and 2 show the two types of DSC plots that were obtained for the ProFile specimens. In all of the DSC plots, the heating curve is shown as a solid line at the bottom of the figure, and the cooling curve is shown as a dashed line at the top of the figure. The lines obtained by extrapolating the baselines adjacent to the peaks show the temperature ranges for the transformations. The other construction lines are used by the computer software to calculate values of enthalpy change ( $\Delta H$ ) and determine onset temperatures for the transformations.

A pair of endothermic peaks can be seen on the heating curve in Figure 1, whereas an unresolved smaller endothermic peak exists on the left shoulder of the main peak at approximately  $10^{\circ}\text{C}$ . These peaks correspond to the initial transformation of martensitic NiTi to R-phase at lower temperatures, followed by transformation at higher temperatures of R-phase to austenitic NiTi, which is completed at approximately  $25^{\circ}\text{C}$ . The area under both peaks represents a total enthalpy change ( $\Delta H$ ) of approximately  $3.3\text{ J/g}$  for the overall transformation from martensitic NiTi to austenitic NiTi. On the cooling curve, there is a broad exothermic peak at approxi-

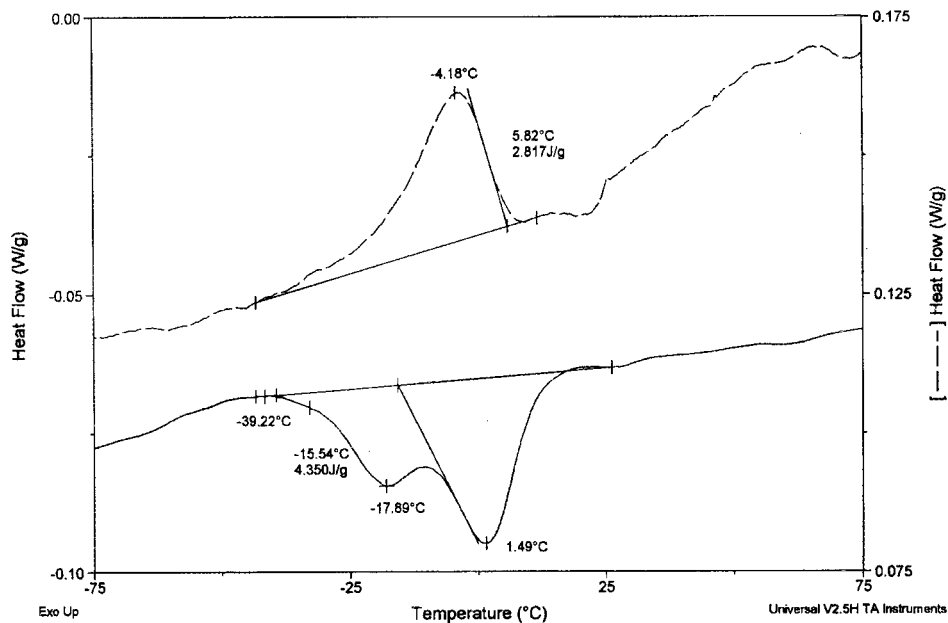


Fig 2. DSC plot for a second ProFile specimen. The solid line is the heating curve, and the dashed line is the cooling curve.

mately 5°C; and the overall enthalpy change of approximately 3.4 J/g also includes a contribution from the unresolved smaller exothermic peak on the left shoulder, i.e. at lower temperatures than the main peak. Note that the vertical scale has been expanded for the heating curve, compared with the cooling curve. The main peak on the cooling curve corresponds to the initial transformation of austenitic NiTi to R-phase, which then transforms at lower temperatures to martensitic NiTi with a much lower enthalpy change than that for the transformation from austenitic NiTi to R-phase.

In Figure 2, for another ProFile specimen, the smaller endothermic peak at approximately  $-18^{\circ}\text{C}$  on the heating curve, corresponding to the initial transformation from martensitic NiTi to R-phase, is now resolved. The second endothermic peak at approximately  $1^{\circ}\text{C}$  corresponds to the subsequent transformation from R-phase to austenitic NiTi. The enthalpy value of 4.4 J/g is applicable to the overall transformation from martensitic NiTi to austenitic NiTi when the sample is heated. For this specimen, the transformation to austenitic NiTi on heating ( $A_f$  temperature) is again completed at approximately  $25^{\circ}\text{C}$ . The interpretation of the cooling curve follows that for Figure 1, with the main exothermic peak at approximately  $-4^{\circ}\text{C}$ , corresponding to the transformation from austenitic NiTi to R-phase. The transformation at lower temperatures from R-phase to martensitic NiTi again appears as an unresolved exothermic peak on the left shoulder of the main peak and has a lower enthalpy change than the transformation from austenitic NiTi to R-phase. The enthalpy change of 2.8 J/g corresponds to the overall transformation from austenitic NiTi to martensitic NiTi when the sample is cooled. Note that both the heating and cooling curves have the same vertical scale in Figure 2.

The other three ProFile specimens had DSC plots that were very similar to Figures 1 and 2. For the five specimens, the enthalpy change for the overall transformation from martensitic NiTi to austenitic NiTi on the heating curve ranged from approximately 3.3 to 4.4 J/g, and the enthalpy change for overall transformation from austenitic NiTi to martensitic NiTi on the cooling curve ranged from approximately 2.8 to 3.6 J/g. The transformation to the austenitic NiTi structure on heating was largely completed for all five specimens at approximately  $25^{\circ}\text{C}$ .

Figure 3 shows a DSC plot for a specimen prepared from the starting wire blanks used to manufacture the ProFile instruments; nearly the same results were obtained for the two specimens that were analyzed. The heating curve contains a clearly resolved first endothermic peak at approximately  $-25^{\circ}\text{C}$  for the transformation from martensitic NiTi to R-phase, followed by a second endothermic peak at approximately  $2^{\circ}\text{C}$  for the transformation from R-phase to austenitic NiTi, which is completed at approximately  $25^{\circ}\text{C}$ . The enthalpy change of 4.8 J/g corresponds to the overall transformation from martensitic NiTi to austenitic NiTi. The cooling curve contains a single resolved exothermic peak at approximately  $-6^{\circ}\text{C}$ , corresponding to the transformation from austenitic NiTi to R-phase. As in Figures 1 and 2, the peak for the subsequent transformation from R-phase to martensitic NiTi is an unresolved left shoulder on the main exothermic peak and has a much lower enthalpy change than the initial transformation from austenitic NiTi to R-phase. The enthalpy change of 3.4 J/g corresponds to the overall transformation from austenitic NiTi to martensitic NiTi. (Note that the vertical scale for the heating curve has been substantially expanded, compared with the scale for the cooling curve.)

Figure 4 shows a DSC plot for a Lightspeed test specimen; very similar results were obtained for the other three samples. The heating curve contains two endothermic peaks at approximately  $-16^{\circ}\text{C}$  and  $2^{\circ}\text{C}$  that correspond to the transformation from martensitic NiTi to R-phase, followed by the transformation from R-phase to austenitic NiTi, respectively. The enthalpy change for the overall transformation from martensitic NiTi to austenitic NiTi is 8.2 J/g. As in the ProFile specimens in Figures 1 and 2, the cooling curve in Figure 4 contains a single exothermic peak at approximately  $-2^{\circ}\text{C}$ , but the extended left shoulder suggests the presence of an unresolved second exothermic peak with a smaller enthalpy change. Accordingly, the cooling curve is assumed to indicate the transformation of austenitic NiTi to R-phase, followed by the transformation at lower temperature from R-phase to martensitic NiTi. The enthalpy change of 2.6 J/g arises from the overall transformation from austenitic NiTi to martensitic NiTi. For the four Lightspeed specimens, the overall enthalpy change on the

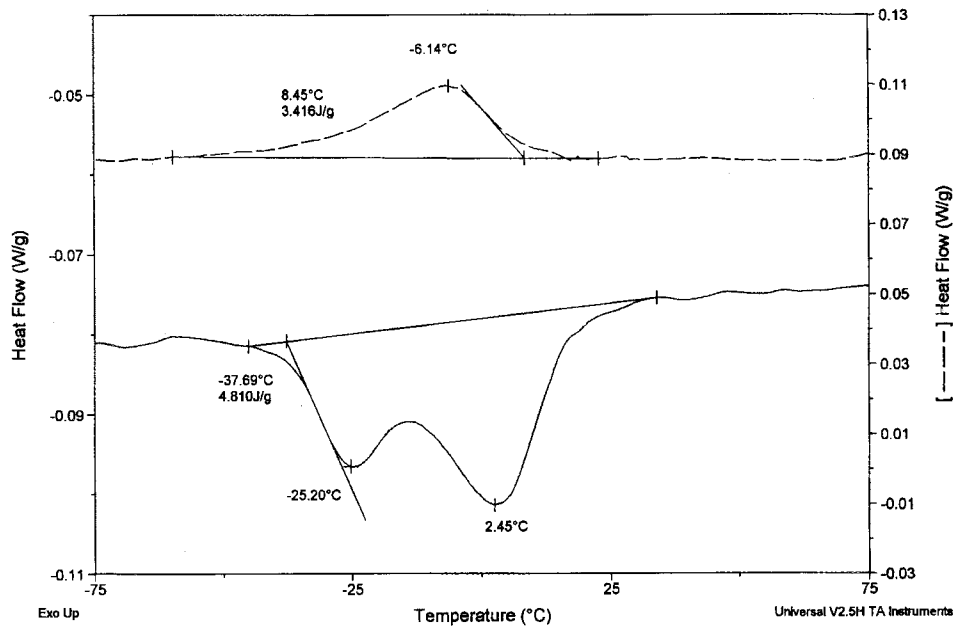


Fig 3. DSC plot for a specimen prepared from the NiTi wire blanks used to manufacture the ProFile rotary instruments. The solid line is the heating curve, and the dashed line is the cooling curve.

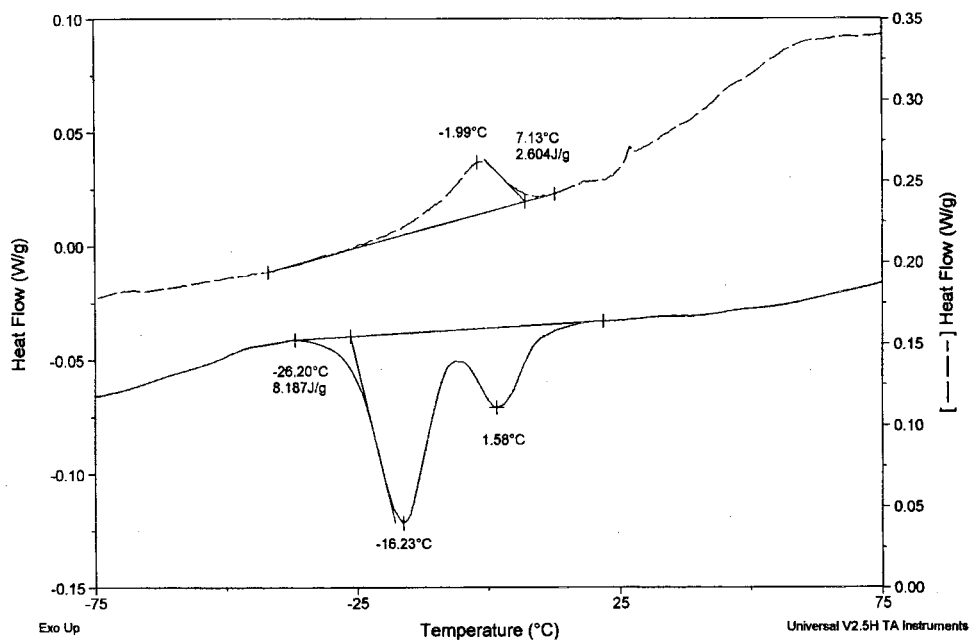


Fig 4. DSC plot for a Lightspeed specimen. The solid line is the heating curve, and the dashed line is the cooling curve.

heating curves ranged from 7.4 to 8.4 J/g, and the overall enthalpy change on the cooling curves ranged from 1.8 to 2.6 J/g. The transformation to the austenitic NiTi structure on heating was completed at 25°C for all four specimens.

The three Quantec specimens, which had an unknown clinical history, had more variable DSC plots than the ProFile and Lightspeed specimens, which were prepared from known as-received instruments. Figure 5 shows the DSC plot for one Quantec specimen; the general appearance of the plots was similar for the other two specimens, although there was substantial variation in the peak temperatures. The heating curve in

Figure 5 contains two clearly resolved endothermic peaks at approximately  $-24^{\circ}$  and  $3^{\circ}\text{C}$  that correspond to the transformation from martensitic NiTi to R-phase, followed by the transformation from R-phase to austenitic NiTi. The enthalpy change of 4.3 J/g is for the overall transformation from martensitic NiTi to austenitic NiTi. The cooling curve contains a single, broad, exothermic peak at approximately  $1^{\circ}\text{C}$ , which is assumed to include both the transformation from austenitic NiTi to R-phase at higher temperatures, followed by the transformation from R-phase to martensitic NiTi because of the long shoulder on the left side of this broad peak. The enthalpy change

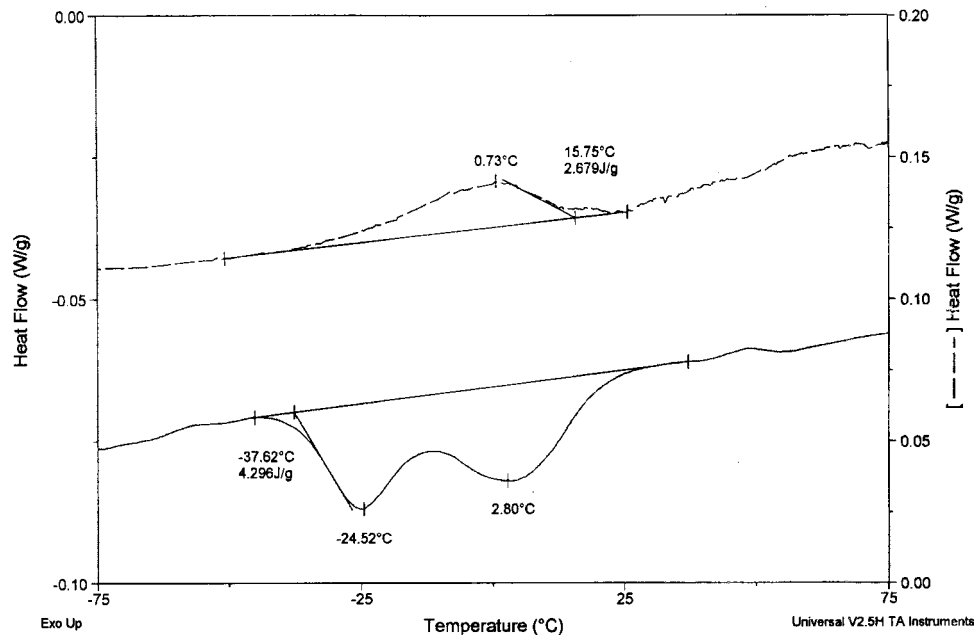


Fig 5. DSC plot for a Quantec specimen. The solid line is the heating curve, and the dashed line is the cooling curve.

TABLE 1. Properties determined from the differential scanning calorimetric (DSC) plots for the three brands of endodontic instruments

Property	ProFile*	Lightspeed	Quantec†
$\Delta H$ (martensitic NiTi to austenitic NiTi) on heating (J/g)	3.3 – 4.9	7.4 – 8.4	4.3 – 7.7
$\Delta H$ (austenitic NiTi to martensitic NiTi) on cooling (J/g)	2.8 – 3.6	1.8 – 2.6	1.6 – 2.7
Peak temperature, martensitic NiTi to R-phase on heating (°C)	-25 – 14‡	-18 – -16	-25 – -9
Peak temperature, R-phase to austenitic NiTi on heating (°C)	1 – 10	2 – 3	3 – 24
Peak temperature, austenitic NiTi to R-phase on cooling (°C)	-6 – +5	-3 – 0	1 – 26
Approximate completion temperature for transformation to austenitic NiTi (°C)	25	25	25 – 50

\* Includes data for instruments and blanks.

† Used instruments.

‡ Not clearly defined for samples from three instruments, i.e. based on samples from two instruments and two wire blanks.

of 2.7 J/g is likewise assumed to correspond to the overall transformation from austenitic NiTi to martensitic NiTi.

The second Quantec specimen had endothermic peak temperatures of  $-12^{\circ}$  and  $19^{\circ}\text{C}$  on the heating curve, with an overall enthalpy change of 5.8 J/g. On the cooling curve, the exothermic peak temperature was  $16^{\circ}\text{C}$  with an overall enthalpy change of 1.6 J/g. The third Quantec specimen had endothermic peak temperatures of  $-9^{\circ}$  and  $24^{\circ}\text{C}$  on the heating curve, with an overall enthalpy change of 7.7 J/g. On the cooling curve, the exothermic peak temperature was  $26^{\circ}\text{C}$  with an overall enthalpy change of 2.6 J/g. Whereas the transformation to austenitic NiTi on heating was nearly completed at  $25^{\circ}\text{C}$  for the Quantec specimen in Figure 5, the temperatures were approximately  $40^{\circ}$  and  $50^{\circ}\text{C}$  for the other two specimens.

Table 1 summarizes the properties determined from the DSC measurements on the three brands of NiTi rotary endodontic instruments. Ranges of the enthalpy changes are provided for the overall forward and reverse transformations between martensitic NiTi and austenitic NiTi on heating and cooling, respectively. Ranges in peak temperatures are listed for the transformations from martensitic NiTi to R-phase and from R-phase to austenitic NiTi on heating and for the transformation from austenitic NiTi to R-phase on cooling. (There were no clearly

defined peaks on the cooling DSC plots for the transformation from R-phase to martensitic NiTi.) Lastly, the approximate completion temperature ( $A_f$ ) is given for the transformation to austenitic NiTi on heating.

## DISCUSSION

The DSC results in Figures 1, 2, and 4 show that the as-received ProFile and Lightspeed rotary endodontic instruments analyzed would be essentially in the completely austenitic NiTi condition at room temperature. These instruments would undergo superelastic behavior during clinical usage, where the imposition of stress causes transformation to martensitic NiTi and the removal of stress (withdrawal of the instrument from the root canal) results in reversible transformation to the original austenitic NiTi structure, unless more than approximately 10% tensile strain takes place (13). By analogy with the DSC results for shape memory NiTi orthodontic wires (11, 16), the NiTi alloy for the ProFile and Lightspeed rotary instruments would be capable of true shape memory under clinical conditions, if the manufacturers performed the necessary processing procedures (15). However, the shape memory property would not be necessary for the clinical use of

# Explore Litigation Insights

Docket Alarm provides insights to develop a more informed litigation strategy and the peace of mind of knowing you're on top of things.

## Real-Time Litigation Alerts



Keep your litigation team up-to-date with **real-time alerts** and advanced team management tools built for the enterprise, all while greatly reducing PACER spend.

Our comprehensive service means we can handle Federal, State, and Administrative courts across the country.

## Advanced Docket Research



With over 230 million records, Docket Alarm's cloud-native docket research platform finds what other services can't. Coverage includes Federal, State, plus PTAB, TTAB, ITC and NLRB decisions, all in one place.

Identify arguments that have been successful in the past with full text, pinpoint searching. Link to case law cited within any court document via Fastcase.

## Analytics At Your Fingertips



Learn what happened the last time a particular judge, opposing counsel or company faced cases similar to yours.

Advanced out-of-the-box PTAB and TTAB analytics are always at your fingertips.

## API

Docket Alarm offers a powerful API (application programming interface) to developers that want to integrate case filings into their apps.

## LAW FIRMS

Build custom dashboards for your attorneys and clients with live data direct from the court.

Automate many repetitive legal tasks like conflict checks, document management, and marketing.

## FINANCIAL INSTITUTIONS

Litigation and bankruptcy checks for companies and debtors.

## E-DISCOVERY AND LEGAL VENDORS

Sync your system to PACER to automate legal marketing.